ELSEVIER

Biophysical Chemistry 57 (1996) 239–251

Biophysical Chemistry

A model for a bistable biochemical trigger of mitosis

C.D. Thron

Department of Pharmacology and Toxicology, Dartmouth Medical School, 7650 Remsen, Hanover, NH 03755-3835, USA

Received 4 January 1995; revised 22 May 1995; accepted 22 May 1995

Abstract

The activation of maturation promoting factor (MPF, cyclin B/Cdc2), which starts mitosis, is modeled as a bistable biochemical switch or trigger. A small, slow parameter change can cause an abrupt transition by a saddle-node bifurcation from a stable steady state of low activity to one of high activity. The switch is not reversed if the parameter change is reversed (hysteresis). The dynamical features necessary for this triggering action are the presence of two stable steady states (low-activity and high-activity), and one unstable steady state. The key biochemical kinetic features of the model are (1) mutual activation by MPF and Cdc25, which makes the activation of MPF effectively autocatalytic, and (2) binding of MPF by Suc1, which inhibits MPF autocatalysis and stabilizes the low-activity steady state until the amount of MPF begins to approach or exceed stoichiometrically the amount of Suc1, then allows strong autocatalysis and full activation. The special virtues of bistable triggering, and the general types of biochemical mechanism which can produce it, are discussed.

Keywords: $p13^{suc1}$; Cdc2; Cdc25; Wee1; Cyclin B; Maturation promoting factor; Cell cycle; Mathematical model

1. Introduction

It is currently believed that mitosis in eukaryotic cells is brought on by activation of a protein kinase (maturation promoting factor, MPF, hereafter called 'M') composed of a catalytic subunit Cdc2 and a positive regulatory subunit cyclin B [1–5]. Cyclin B is biosynthesized and combines with Cdc2, and the dimer is phosphorylated to an inactive form ('P') by the tyrosine kinase Wee1. The inactive form P accumulates apparently under controls which prevent premature activation. It is activated by Cdc25, a highly specific tyrosine phosphatase. Small amounts of M promote formation of larger amounts ('amplification') from an endogenous precursor [6], and this suggests that activation of M is autocatalytic. This conclusion seems supported by the weight of evidence, although it has been questioned [1]. Cdc25 is itself activated by M, and this could account for the autocatalysis.

Several recent mathematical models of the cell cycle assume that this autocatalysis generates oscillations which drive repeated mitosis [7–16]; and it has recently been suggested [15] that the protein Suc1 ($p13^{suc1}$), which strongly binds MPF and blocks mitotic activation of Cdc2 in cell-free systems [17,18], may play a crucial dynamical role in the generation of these oscillations. However it has been emphasized [10,12–14] that autonomous oscillation is probably not the usual mode of cell cycle operation, and that progress through the cell cycle is regulated by 'checkpoint' controls which ensure, for example, adequate cell size and complete DNA replication before starting mitosis. In such cells the auto-

SSDI 0301-4622(95)00075-5

catalytic process probably functions mainly as a switch under checkpoint control. The role of Suc1 therefore must be re-examined in relation to this switching action, as opposed to the generation of oscillations. The purpose of the present paper is to examine the autocatalytic activation as part of a biochemical switch or trigger, rather than a limit cycle oscillator, and to clarify the dynamics of the switching or triggering and the implications for the biochemical kinetics and the role of Suc1.

Roman letters (M, P, etc.) will be used to denote substances, italic letters (M, P, etc.) concentrations.

2. A model of the mitotic trigger

In the model proposed previously [15] the protein Suc1 (hereafter called B), which binds M and inhibits autocatalysis, was assigned a role which was dynamically essential for the generation of oscillations. This was based on the fact that Suc1 binds strongly to MPF and blocks mitotic activation and tyrosine dephosphorylation of Cdc2 in cell-free systems [17,18]. The model proposed here (Fig. 1; Table 1) differs primarily in that it allows for no cyclin biosynthesis or degradation, and considers only the activation and inactivation of M when the total concentration $Q(=M+P)$ is constant. There is only one state variable (M), and no oscillations are possible. In addition, the mechanism of M autocatalysis is slightly different. In the previous model, the activation of M was attributed to a complex MD (a trimer of Cdc2/cyclin B/Cdc25, as proposed by Galaktionov and Beach [19]), which catalyzed the activation of M. The present model omits this complex and instead adopts a suggestion of Zheng and Ruderman [20] (see also Discussion) that the low-activity interphase form of Cdc25 (D^0) activates P to M slowly, then the M produced by this reaction converts Cdc25 to the active form (D^*), which activates more M rapidly. M binds to B (Suc1), and only unbound M (M_f) is effective in activating Cdc25. Bound and unbound M are assumed to have the same rate constant for tyrosine phosphorylation (reverse of activation). The model is summarized in Table 1. The corresponding MD complex model (discussed in [15]) is also of the form in Fig. 1, and is probably similar dynamically.

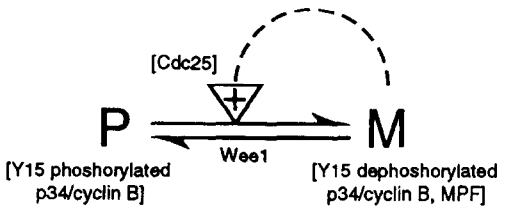

Fig. 1. A general model of the mitotic trigger. M enhances its own activation.

In the present model, the rate of formation of M depends on both the inactive (D^0) and the active (D^*) forms of Cdc25, and on the amount of inactive form P:

$$F_M = eD^0P + fD^*P = [e(D - D^*) + fD^*](Q - M), \quad (1)$$

where D is the total of D^0 and D^*, Q is the total of M and P, and e and f are constants. D and Q are

Table 1
A model of the mitotic trigger

1. Tyrosine 15-phophorylated Cdc2/cyclin B is slowly activated by the low-activity interphase form of Cdc25 to MPF (tyrosine 15-dephosphorylated Cdc2/cyclin B)	$P \xrightarrow{D^0} M$
2. The same is rapidly activated by the high-activity hyperphosphorylated form of Cdc25	$P \xrightarrow{D^*} M$
3. Suc1 binds MPF reversibly (M_f, B_f = unbound M, B)	$B_f + M_f \rightleftarrows MB$
4. Cdc25 (low-activity interphase form) is activated by MPF to the high-activity hyperphosphorylated form	$D^0 \xrightarrow{M_f} D^*$
5. Cdc25 is deactivated	$D^* \rightarrow D^0$
6. MPF is inactivated by Wee1	$M \rightarrow P$

assumed to be constant, and M binds to Suc1 (B) according to

$$K = \frac{M_f B_f}{[MB]} = \frac{M_f B_f}{M - M_f} = \frac{M_f[B - (M - M_f)]}{M - M_f}, \tag{2}$$

where M_f is M not bound to B, B_f is B not bound to M, $M = M_f + [MB]$ and B is a constant, the total of $B_f + [MB]$. Solving for M_f gives

$$M_f = \frac{-(B - M + K) + \sqrt{(B - M + K)^2 + 4KM}}{2}. \tag{3}$$

The two forms of D are assumed to be in a steady state, with the rate of activation of D^0 to D^* proportional to M_f.

$$K_D = \frac{D^*}{M_f D^0} = \frac{D^*}{M_f(D - D^*)}, \tag{4}$$

so

$$D^* = \frac{K_D M_f D}{1 + K_D M_f}. \tag{5}$$

Substituting in Eq. 1:

$$F_M = \left[e + (f - e)\frac{K_D M_f}{1 + K_D M_f}\right] D(Q - M). \tag{6}$$

Since binding of M to B reduces M_f, it reduces D^* (Eq. 5) and inhibits the autocatalytic activation of M. However if M increases beyond the stoichiometric binding capacity of B then M_f tends to rise relatively rapidly with increasing M, and this has an important effect on the dynamics, as noted previously [15], and as will be seen below.

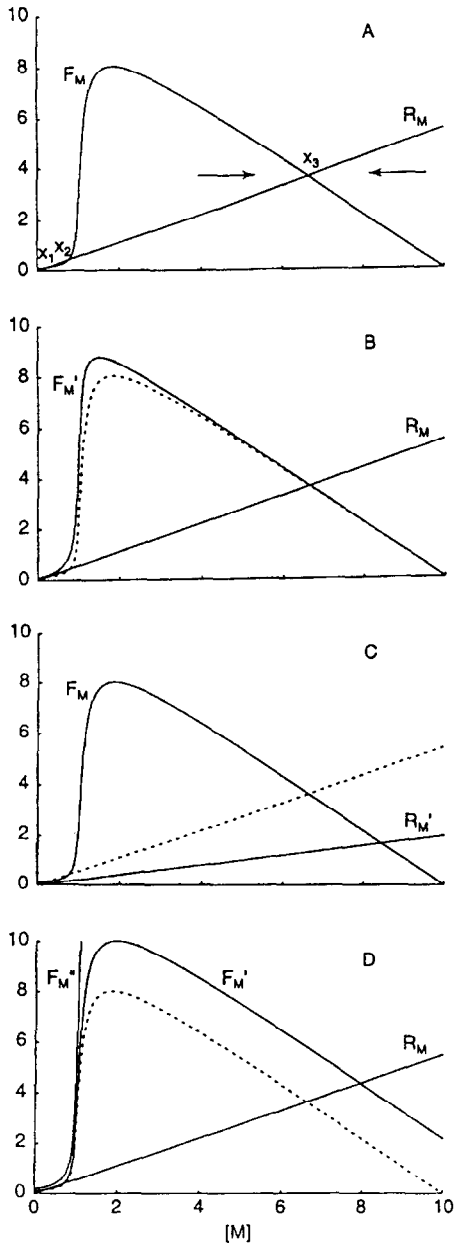

Fig. 2. (A) Rate of M activation $\mathbf{F}_M$ and inactivation $\mathbf{R}_M$ (Eqs. 3 and 7). The curves intersect at the fixed points (steady states), two stable ($\mathbf{x}_1$, $\mathbf{x}_3$) and one unstable ($\mathbf{x}_2$). Arrows indicate the direction of change of [M] toward the stable fixed point $\mathbf{x}_3$. At [M] levels where $\mathbf{F}_M > \mathbf{R}_M$, [M] tends to increase, and where $\mathbf{F}_M < \mathbf{R}_M$, [M] tends to decrease. Parameter values: $e = 0.01$, $D = 1$, $f = 1.1$, $Q = 10$, $K_D = 10$, $B = 1$, $K = 10^{-3}$ and $w = 0.55$. (B) Triggering by increased activation of Cdc25 (K_D increased to 30 in Eq. 6). The dashed line is Curve $\mathbf{F}_M$ from Fig. 2A. The altered rate of activation $\mathbf{F}'_M$ no longer intersects $\mathbf{R}_M$ at low [M], and there is no stable low-activity steady state. (C) Triggering by inhibition of Wee1 (w decreased to 0.2). $\mathbf{R}'_M$ no longer intersects $\mathbf{F}_M$ at low [M]. (D) Triggering by increase of total active plus inactive cyclin B/Cdc2 complex ($M + P = Q$), e.g. by cyclin B biosynthesis. With Q increased to 12, $\mathbf{F}'_M$ is raised, still intersects $\mathbf{R}_M$ at low [M], and intersects the abscissa off-scale at [M] = 12. With $Q = 30$, $\mathbf{F}''_M$ is greatly raised (lies mostly off-scale) and no longer intersects $\mathbf{R}_M$ at low [M].

With a linear inactivation rate R_M, and an activation rate given by Eq. 6, the differential equation for the model is

$$\frac{dM}{dt} = F_M - R_M$$

$$= \left[e + (f-e)\frac{K_D M_f}{1 + K_D M_f} \right] D(Q-M) - wM, \tag{7}$$

where M_f is unbound M, given by Eq. 3, and w is the inactivation rate constant, assumed to be the same for M_f and for M bound to B.

Experimental values for the parameters of Eq. 7 are not presently available. For illustration, nominal values without units are assigned here. Since no units are specified the relation of these values to real biological values is indeterminate. System behavior depends only on the relative parameter values, and these have been set to produce various types of dynamical behavior. The effects of several different parameter choices can be seen in Figs. 2 and 3, and 8; and others can be predicted from Eqs. 3 and 7. The applicability of the model to any particular real system would depend on an appropriate choice of parameter values.

With the assumed parameter values, Fig. 2A shows the activation and inactivation rates (F_M, R_M) as a function of M. At M levels where $F_M > R_M$, M tends to increase, and where $F_M < R_M$, M tends to decrease, as shown by the arrows. The points where F_M and R_M intersect ($\mathbf{x}_1$, $\mathbf{x}_2$, $\mathbf{x}_3$) are 'fixed points,' where there is no tendency for M to change. From the direction of change of M, as determined by the relative magnitudes of F_M and R_M, it can be seen that M changes away from $\mathbf{x}_2$ and toward $\mathbf{x}_1$ and $\mathbf{x}_3$; therefore $\mathbf{x}_1$ and $\mathbf{x}_3$ are stable fixed points and $\mathbf{x}_2$ is an unstable fixed point.

This system can be triggered to switch abruptly from one stable steady state to the other (Fig. 2B–D). Consider a system initially at the low-activity stable steady state. An increase in K_D (corresponding to activation of Cdc25) moves the activation rate curve upward (F'_M, Fig. 2B), so that it no longer intersects R_M in the low-activity range. There is no longer a stable low-activity steady state. That value of M now lies in the region of attraction of the high-activity stable steady state, and therefore the system shifts to the high-activity state directly, producing abrupt activation. The triggering is due to the change in the number of fixed points, mathematically a saddle-node bifurcation [21].

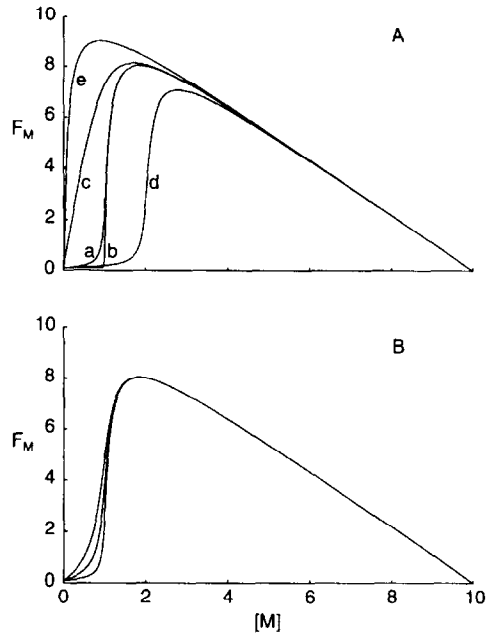

Fig. 3. (A) Factors affecting the rate of M activation $\mathbf{F}_M$ (Eq. 6). In curve **a**, $e = 0.01, D = 1$, $f = 1.1$, $Q = 10$, $K_D = 10$, $B = 1$, and $K = 10^{-3}$. Increase in binding affinity (curve **b**, $K = 10^{-5}$) makes the rise in F_M sharper. Decrease in binding affinity (curve **c**, $K = 10^{-1}$) abolishes the upward curvature. Increase in the amount of binding substance (curve **d**, $B = 2$, $K = 10^{-3}$) displaces the rapid upward curvature to higher [M]. Elimination of binding substance (curve **e**, $B = 0$) abolishes the upward curvature. (B) Effect of competitive binding to B of the inactive form P. If P binding is appreciable, the upward curvature of $\mathbf{F}_M$ is reduced or abolished. In the three curves, from left to right, the PB dissociation constant (corresponding to the MB dissociation constant K in Eqs. 2–3) is 1, 3, and 100, respectively.

Fig. 2C and 2D show bifurcation and triggering by a decrease in the rate constant w for M inactivation (inhibition of Wee1), and by an increase in the total concentration Q (from biosynthesis or addition of cyclin), respectively. In each case the key event is the loss of contact between F_M and R_M at the low-activity stable steady state.

Fig. 3A shows the importance of binding of M to B for abrupt triggering. Elimination of B (curve **e**) or decrease in binding affinity (curve **c**) eliminate the

region of upward curvature in F_M, so that it is no longer possible (with linear R_M) to have both low-activity and high-activity fixed stable steady states ($\mathbf{x}_1$ and $\mathbf{x}_3$, respectively, in Fig. 2A), and therefore abrupt triggering is impossible. Increase in binding affinity (curve **b**) makes the rise in F_M more abrupt. The rapid rise in F_M occurs approximately where M begins to exceed B stoichiometrically, as can be seen by comparing curves **a** and **b** ($B = 1$) with **d** ($B = 2$).

As previously noted [15], Suc1 binds both tyrosine 15-phosphorylated and -dephosphorylated Cdc2. In the model, if P binds to B appreciably, the upward curvature of F_M is reduced or abolished (Fig. 3B), eventually making impossible (with linear R_M) the three intersections required for bistability. Essentially this is because competitive binding of P (or any other substance) reduces the apparent affinity of M for B (cf. curve **c**, Fig. 3A). Fig. 3B suggests that for bistable switching the relative affinity of P must be weaker than that of M by a factor of at least 10^4; but computations show that with a smaller value of K_D ($= 0.1$), which gives a higher effective reaction order of autocatalysis, bistable switching is possible with an affinity ratio as low as 250. There appear to be no quantitative data on the relative affinity of Suc1 for tyrosine 15-phosphorylated and -dephosphorylated Cdc2.

If R_M is nonlinear then upward curvature of F_M may not be required to get two stable fixed points, as illustrated in Fig. 4. A nonlinear R_M might be more typical of the effect of Wee1 than is the linear R_M in

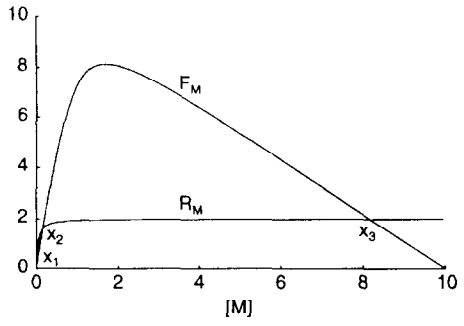

Fig. 4. Rate of M activation $\mathbf{F_M}$ with low B binding affinity (curve **c** from Fig. 3A) and rate of inactivation $\mathbf{R_M}$ with saturable kinetics: $R_M = 2[M]/(0.04+[M])$. There are stable fixed points at low ($\mathbf{x}_1$) and high ($\mathbf{x}_3$) activity, and an unstable fixed point ($\mathbf{x}_2$).

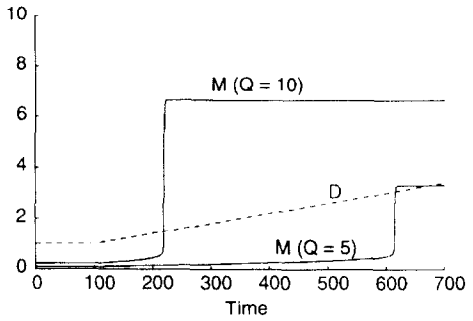

Fig. 5. Triggering of the model (Eq. 7) on a slow increase in D, with different total amounts Q. The model is initially in a stable steady state. At time 100, a gradual increase in D begins (dashed line) and leads to a delayed abrupt rise in M. With $Q = 10$, the required increase in D is about 40%; with $Q = 5$, the required increase is about 195%.

Fig. 2, since Wee1 activity decreases in M phase [22–24], and therefore the increased M in M phase will not produce a proportional increase (and may even produce a decrease) in R_M.

Because of the mode of switching by saddle-node bifurcation, activation of M does not require a sharp pulse or signal, but can be triggered by a slight and slow parameter change. Fig. 5 shows the response of the model (Eq. 7) to a slow rise in D. When D reaches a threshold, a bifurcation occurs (cf. Fig. 2B–D) which produces an abrupt rise in M. The threshold occurs where the curve of F_M is just tangent to the curve of R_M (cf. Fig. 2). At the point of tangency F_M (Eq. 6) is equal to R_M ($= wM$) and the slopes are equal ($\partial F_M/\partial M = \partial R_M/\partial M = w$). The threshold value for D can be found by solving these two equations simultaneously for M and D. Since M is determined only implicitly, the solution must be obtained numerically.

Activation is slow at D levels barely above threshold, so in Fig. 5 D rises slightly above the theoretical threshold before the rapid rise in M actually occurs. At the lower level of Q the threshold triggering level of D is higher and the rise in M is smaller. This higher D threshold may inhibit triggering when the level of Q is too low to produce a decisive rise in M; but this is apparently not a strict 'checkpoint' control, since it may only delay, rather than fully prevent, triggering at suboptimal Q levels.

The activation of D in Fig. 2B corresponds to the activation of Cdc25, which triggers mitosis in human

and *Xenopus* cells, where total Cdc25 remains approximately constant (see [25] for references). The increase in D in Fig. 5 would correspond to the case of yeasts, where mitosis appears to be driven by periodic increases in total Cdc25 [26,27].

3. The effect of turnover of M and P

The foregoing has treated the mitotic switch as a closed system. This section examines the relation of the closed model (Eq. 7) to previous oscillatory models. Previous models (e.g. [15]), in order to generate oscillations, have assumed that there is continuous biosynthesis and degradation of cyclin B, hence of M and P. This makes a fundamental change in the dynamics. The system then has two state variables, M and P. If M is biosynthesized (i.e. by cyclin biosynthesis) at a constant rate i, and degraded at a rate gM, then the system equations are

$$\frac{dP}{dt} = -\left[e + (f-e)\frac{K_D M_f}{1 + K_D M_f}\right]DP + wM, \quad (8)$$

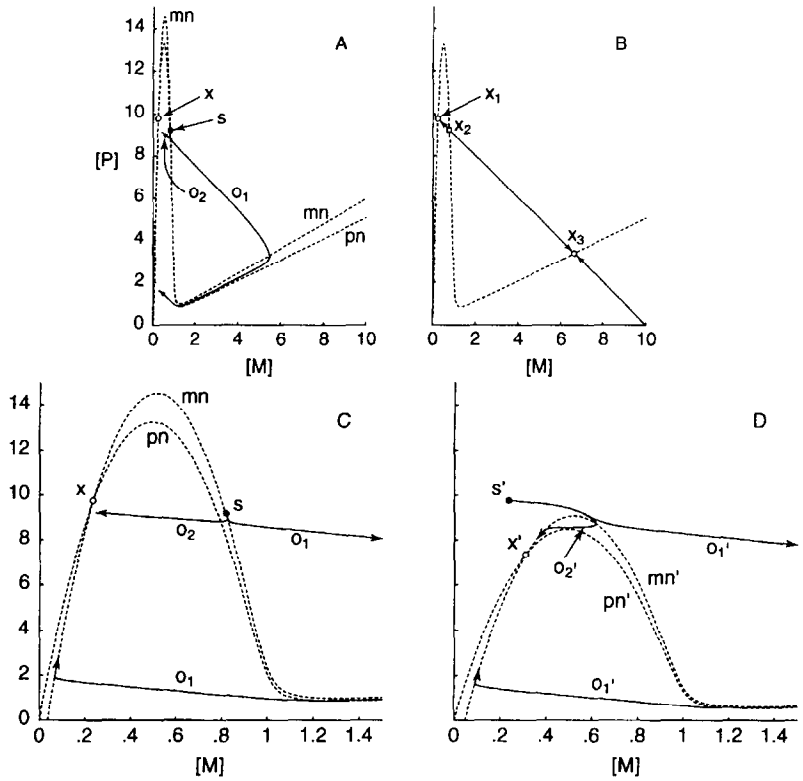

Fig. 6. Phase plane plots for a system with biosynthesis and degradation of the components (Eqs. 8–9, parameters as in Fig. 2A, with $g = 0.1$, $i = 0.0237461$). (A) (see also C) The M and P nullclines (dashed curves **mn, pn**) intersect at a single stable fixed point (**x**). The turnover rate is low, so the nullclines lie very close together. The system is excitable: on displacement of the state vector (along the diagonal $M + P = Q$, which is not shown) to the point s just beyond the M nullcline, the orbit follows close to the M nullcline for a short distance, then turns abruptly left or right, making either a large excursion ($\mathbf{o}_1$) or a more direct return ($\mathbf{o}_2$) to the stable fixed point x. (B) Corresponding phase plane plot of the closed system (Eq. 7). The M and P nullclines superimpose. M and P are constrained to add to Q, so the direction of the vector field is uniformly $-45°$ above the common nullcline, and $+135°$ below it. The diagonal line contains all the orbits for $M + P = 10$. Its intersections with the common nullcline are the three fixed points of Fig. 2A, two stable ($\mathbf{x}_1$, $\mathbf{x}_3$) and one unstable ($\mathbf{x}_2$). Arrows show the orbits converging to $\mathbf{x}_1$ and $\mathbf{x}_3$. (C) Part of A with expanded M scale. (D) Triggering by a parameter change. The figure shows the new nullclines, after increasing D to 1.564. An orbit $\mathbf{o}_1'$ tarting at s' (identical to the original stable point **x** in Fig. 6A) passes close to the new M nullcline, then makes a large excursion (off scale), with activation of M comparable to that in A, before going to the new stable fixed point x'. With a slightly smaller value of D (1.563) the nullclines (not shown) are almost unchanged, but the orbit ($\mathbf{o}_2'$) does not make a large excursion.

and

$$\frac{dM}{dt} = i + \left[e + (f - e)\frac{K_D M_f}{1 + K_D M_f} \right] DP - (w + g)M. \quad (9)$$

This system, with small i and g, may be compared with the model of Eq. 7, in order to see the effect of M turnover (cyclin synthesis and degradation) on the dynamics. Fig. 6A and 6C show the phase plane plot for this system, with M and P nullclines **mn** and **pn**, respectively. For comparison, Fig. 6B shows the corresponding phase plane plot of the closed system, Eq. 7.

In the closed system (Fig. 6B), the M and P nullclines superimpose. M and P are constrained to add to Q; so the direction of the vector field is uniformly $-45°$ above the common nullcline, and $+135°$ below it. The diagonal line shown contains all the orbits for $M + P = 10$ and it intersects the common nullcline at the three fixed points of Fig. 2A, two stable ($\mathbf{x}_1$, $\mathbf{x}_3$) and one unstable ($\mathbf{x}_2$).

When turnover is added (Fig. 6A,C), the M and P nullclines separate, except for a single intersection (**x**) where $i = gM$ in Eq. 9. In this case the values of i and g were chosen so that the net rate of change due to turnover was zero at the lower stable fixed point of Eq. 7; therefore this is the intersection point of the nullclines, and the stable steady state **x** is identical to the point $\mathbf{x}_1$ in the closed system (Fig. 6B). On either side of this point in the open system there are extremely thin wedges of territory between the nullclines (Fig. 6C) where the direction of the vector field is in the first or third quadrant (up-right or down-left); and elsewhere the vector field is no longer uniformly $-45°$ or $+135°$. This makes possible rotary or spiral motion about **x**.

If the closed system (Fig. 6B) is at rest at the lower fixed point $\mathbf{x}_1$, then on displacement of the system along the diagonal $M + P = Q$ beyond the unstable fixed point $\mathbf{x}_2$ the system goes on spontaneously to the upper fixed point $\mathbf{x}_3$, and does not return to $\mathbf{x}_1$. On similar displacement of the open system (Fig. 6A,C) to the point **s** just beyond the M nullcline, the orbit follows close to the M nullcline for a short distance, then turns abruptly left or right, making either a large excursion ($\mathbf{o}_1$) with substantial activation of M before returning to the stable fixed point **x**, or a more direct return ($\mathbf{o}_2$) to **x**. This potential for a large excursion makes this what is called an 'excitable' system.

Theoretically, the open system has orbits intermediate between $\mathbf{o}_1$ and $\mathbf{o}_2$, but it was not possible to produce any. The starting points for $\mathbf{o}_1$ and $\mathbf{o}_2$ differed by less than 1 part in $8 \cdot 10^6$; so for practical purposes the excitability is all-or-none, at least for these parameter values. The closed system, of course is strictly all-or-none, always going to one stable state or the other.

The large excursion $\mathbf{o}_1$ in the open system approaches the nullclines, where the rates of change of M and P are slow. Therefore if the turnover rate is very slow this orbit may closely resemble the switch of the closed system to the upper stable fixed point, differing only in having a slow drift away from its upper extremum, which eventually leads to a return to the stable fixed point **x**.

Fig. 6D shows that an increase in the parameter D can trigger a large excursion in the open system initially at rest at the stable fixed point **x** in Fig. 6A,C. An increase in D can change the nullclines from those in Fig. 6A to those in Fig. 6D. An orbit $\mathbf{o}'_1$ starting at **s**′, which is identical to point **x** in Fig. 6A,C, passes close to the new M nullcline, then makes a large excursion, with activation of M, before going to the new stable fixed point **x**′. If D is very slightly (0.06%) less, the orbit from **s**′ makes no large excursion; so the triggering by D is effectively all-or-none (for these parameter values), though theoretically not strictly so. However, the system now shows 'accommodation': if D changes slowly, then the state vector will tend to follow the stable fixed point more or less closely, and will not undergo a large excursion. Accommodation may make the system fail to trigger on a slowly-changing parameter. However if triggering occurs it is essentially irrevocable, because once the system has started on a large excursion it soon enters the strongly autocatalytic region of phase space, where it continues on a large excursion even if the parameter change is reversed.

If i is increased, the intersection of the nullclines moves and becomes unstable, the system undergoes Poincaré–Andronov–Hopf ('Hopf') bifurcation [21], and a stable limit cycle appears. Careful computations show that (with these parameter values) the stable limit cycle appears slightly before the fixed

point becomes unstable; so the Hopf bifurcation is subcritical, and there are no oscillations of small amplitude. Even if the bifurcation were supercritical, the vector field is essentially that of an excitable system, so the oscillations (with exceedingly rare exceptions) are either small or of full amplitude, and oscillations of intermediate amplitude practically never occur. To prevent repetitive mitosis, the Hopf bifurcation must be reversed after the first large excursion; and if the Hopf bifurcation is subcritical then repetitive cycling may persist after restoring stability of the fixed point.

4. Discussion

The model illustrated in Fig. 2A–D is a bistable system which can be triggered by a saddle-node bifurcation. It has long been recognized (e.g. [28]) that a bistable biochemical system can function as a biochemical switch. Mathematical models have been discussed by Tyson [29] and Edelstein-Keshet ([30], pp. 285–287), with references to the earlier literature. Other authors [31–33] have proposed that bistable systems translate continuous chemical gradients into the discontinuous patterns of embryonic development. Bistable systems are also well known in chemical engineering ([34], pp. 18–24; 147 ff.). Such models have several important features. First, they can be triggered by a slow parameter change,

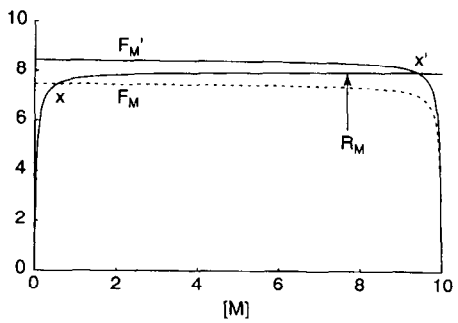

Fig. 7. A biochemical switch based on zero-order ultrasensitivity. Curves $\mathbf{F_M}$, $\mathbf{R_M}$: rates of activation and inactivation of M; **x** fixed point at low activation. A small parameter change shifts curve $\mathbf{F_M}$ to $\mathbf{F'_M}$, with fixed point **x'** at high activation. Under all conditions there is just one fixed point, which is stable, and there is no bifurcation.

and do not require to be driven by a pulse or step. This property might be taken to differentiate a 'trigger' from a 'switch.' Second, they switch in an all-or-none fashion from one steady state to the other, without stopping at any intermediate state. Third, they show hysteresis; that is, a parameter change which triggers a change from one stable steady state to the other does not, when reversed, restore the original steady state. A somewhat larger parameter change in the reverse direction is required to switch back the original steady state. Hysteresis can make the switching 'irrevocable' or, more precisely, difficult to arrest or reverse. These properties, adding up to irrevocable all-or-none switching by a slowly-changing signal, are characteristic of a bistable switch or trigger, and are obviously highly suited to the task of starting a process like mitosis, where a partial or vacillating commitment would undoubtedly be catastrophic.

In contrast to the bistable trigger, Fig. 7 shows a switching mechanism based on a sensitive balance between saturable rates of activation and inactivation, a mechanism called 'zero-order ultrasensitivity' by Goldbeter and Koshland [35]. The quite different model of Okamoto and Hayashi [36] can be graphed similarly. Over most of the range of M in Fig. 7, the processes of activation and inactivation are both very near their maximum velocity, with zero-order kinetics. A small change in one of the maximum velocities can shift the intersection (i.e. the fixed point) from almost complete inactivation (**x**, Fig. 7) to almost complete activation (**x'**). Unlike the model of Fig. 2, it is possible for this system, with an intermediate parameter change, to have a fixed point at intermediate values of M. Furthermore, activation is not irrevocable: if a parameter change causes activation, then reversing that parameter change causes inactivation; so repetitive switching ('chattering') may occur if the parameter hovers at threshold. The same liability to intermediate values and chattering occurs in a switch made up of a succession of cooperative steps [37], which can generate a very large change in the last step in response to a very small change in the first. Such mechanisms may be useful for some biochemical switching, as in logic networks [38] where they are driven by strong signals, but they may not be reliable for generating a full and irrevocable commitment in response to a

slow, small, or vacillating signal. Lewis et al. [31] have noted their unsuitability, on similar grounds, for triggering the events of embryonic morphogenesis.

The dynamical feature necessary for a bistable trigger is the presence of two stable fixed points ($\mathbf{x}_1$ and $\mathbf{x}_3$ in Fig. 2A), where F_M crosses R_M from above downward as M increases. It is obvious from Fig. 2A that these two downward crossings require an intervening upward crossing of R_M by F_M, which makes an unstable fixed point $\mathbf{x}_2$ (F_M and R_M might conceivably coincide over a finite range of M in some cases, but this is not likely, and the following arguments can be adapted to that case). An unstable fixed point (or range) is therefore a necessary feature in a bistable switch.

At an unstable fixed point, $\partial F_M/\partial M \geqslant \partial R_M/\partial M$, with strict inequality in the neighborhood of the fixed point; so either $\partial F_M/\partial M > 0$ or $\partial R_M/\partial M < 0$ near the fixed point. The first of these inequalities would indicate that the formation of M from P is effectively either autocatalytic or substrate-inhibited (since $P + M$ is constant, $\partial F_M/\partial P < 0$ implies $\partial F_M/\partial M > 0$); and the second inequality would likewise indicate that the reverse reaction is effectively either autocatalytic or substrate-inhibited. In all cases, a necessary biochemical kinetic feature for a bistable switch is either a process which is effectively autocatalytic or one that is effectively substrate-inhibited. Through these mechanisms, M or P tends to increase its own net rate of formation, in contrast to the usual law of mass action, by which a substance tends to increase its own net rate of removal, as in the term $-wM$ in Eq. 7.

Since M may affect (mathematically) both activation and inactivation in ways that may increase or decrease its net rate of activation, the stability of a fixed point depends on the directions and relative strengths of these effects. The appropriate measures of these strengths are the orders of reaction [39]. For this purpose, the orders of reaction can be defined as $\phi_M = \partial \log F_M/\partial \log M$ and $\rho_M = \partial \log R_M/\partial \log M$ [40,9,41,15]. For example, if $F_M = kM^n$ then $\phi_M = n$, as is easily verified. If F_M is not a power of M, then the reaction order is not a constant but is M-dependent. For example, with Michaelis–Menten kinetics $F_M = V_{max}M/(K_M + M)$ and $\phi_M = K_M/(K_M + M)$, a function which approaches 1 when M is small, and approaches 0 when M is large, as the reaction order of Michaelis–Menten kinetics is well known to do.

At an unstable fixed point $\partial F_M/\partial M \geqslant \partial R_M/\partial M$, as already noted; and since $F_M = R_M$ it follows that $(M/F_M)(\partial F_M/\partial M) \geqslant (M/R_M)(\partial R_M/\partial M)$, i.e. that $\phi_M \geqslant \rho_M$ at the unstable fixed point, with strict inequality in the neighborhood of the fixed point. For a bistable switch or trigger the biochemical kinetic mechanism must be one that is capable of giving autocatalysis with a reaction order higher than that of inactivation ($\phi_M > \rho_M$) in the neighborhood of the unstable fixed point, for some choice of parameter values. In addition, and with the same parameter values, it must satisfy the opposite inequality ($\phi_M < \rho_M$) at M values near the two stable fixed points. Therefore at least one of the reaction orders (ϕ_M, ρ_M) must be M-dependent, and the reaction order difference $\phi_M - \rho_M$ must take on negative, positive, and negative values in succession as M increases.

In the model of Fig. 2 and Eq. 7, $\rho_M = 1$, and ϕ_M is M-dependent. The latter logarithmic derivative is rather complicated, but the M-dependence of the reaction order can be explained qualitatively. As M approaches 0, F_M approaches eDQ (reaction order 0), and $\phi_M < \rho_M$. When M is large, F_M approaches $fD(Q - M)$ (reaction order < 0), and again $\phi_M < \rho_M$. At intermediate M, if e and K_D are small, and $M \ll Q$, then F_M may approach $fDQK_DM_f$, and since M_f is an upward-curving function of M, with $\partial \log M_f/\partial \log M > 1$ [15], a suitable choice of parameters will give F_M a reaction order > 1 (i.e. $\phi_M > \rho_M$) at intermediate values of M.

The requirement that $\phi_M > \rho_M$ at the unstable fixed point of a bistable system is obviously very similar to one of the requirements for oscillations in the previous model ([15], inequality 8b). Unlike the present model, that model assumed that the rate of autocatalysis was directly proportional to M_f. However biochemical catalysis generally depends on formation of an activated form of an enzyme, of which the total amount is limited. To take this into account, the catalytic effect in the present model is limited to a fixed maximum, i.e. is saturable (Eq. 5). This saturability tends to lower ϕ_M, and in that way works against bistability.

Other biochemical mechanisms can generate the required sequence of negative, positive, and negative reaction orders. The term $K_DM_f/(1 + K_DM_f)$ in

Eq. 7 might be replaced by M^n, with $n > 1$, for example. Alternatively, the rate of inactivation R_M might have saturable (Michaelis–Menten) kinetics, as illustrated in Fig. 4. A similar R_M curve could result from a limited rate of supply of a co-substrate, such as ATP, or if only bound M (MB), and not M_f, were inactivated. If M acts to inhibit Weel, as has been suggested [22–24], then R_M may show substrate inhibition. In that case the curvature of R_M could make possible three fixed points for a bistable switch with a linear F_M without autocatalysis. In many cases it is easier to demonstrate the three fixed points graphically (cf. Fig. 4) than to prove the sequence of reaction orders, but the rule for reaction orders helps to suggest what is needed in the way of biochemical mechanisms and kinetics.

Previous models of the cell cycle have led to a somewhat different model of the mitotic trigger. Those models were made oscillatory to model repetitive mitoses; and for triggerable mitosis the model parameters were adjusted to stabilize the system. The result was an excitable system like those often used to model electrically-excitable nerve and muscle membranes [42,43]. But those excitable systems are typically activated by a sharp displacement of the state vector, i.e. a voltage pulse; and it is not obvious how a suitable bolus of MPF might be generated in the system considered here. At least some signals for cell division, e.g. increase in cell size or hormonal change, must be quite slow; and an excitable system, which shows accommodation and may therefore fail to trigger on such a slowly-changing signal, may not be a good model for the mitotic trigger. In contrast, the closed system (Eq. 7, Figs. 2 and 3) requires no MPF bolus, and can be triggered by a slow parameter change (Fig. 5) (FitzHugh has also considered a bistable model of the nerve membrane with triggering by saddle-node bifurcation [44]).

If nevertheless there is turnover of M (and indirectly of P), it has two effects: on one hand the turnover flux has a buffering effect that tends to stabilize the fixed point and produce accommodation; but on the other hand it also tends to determine the location of the fixed point, and may place it in a strongly autocatalytic region of phase space, where the fixed point is unstable, and oscillations appear. In the case where the fixed point is stable, the system might trigger on a slow parameter change (Fig. 6D) if accommodation is too sluggish to keep the system near the changing low-activity stable steady state. Unlike the closed system (Eq. 7, Figs. 2 and 3), this system activates only transiently, and soon returns to a low-activity steady state. On the other hand, Hopf bifurcation provides a non-accommodating mode of activation, but this is followed by recovery and repetitive activation (oscillations) unless the bifurcation is reversed. Hopf bifurcation with persistent oscillations might be a model for the appearance of repetitive mitoses in malignant cells; and from a therapeutic point of view it is of some interest that the Hopf bifurcation can be reversed, and the oscillations stopped, by a change in parameters (e.g. the ratio g/i) which does not disable the excitability or the triggerability by a sufficiently fast parameter change. This would suggest that uncontrolled repetitive cell division could be stopped without impairing physiological signal-driven cell division. However if the Hopf bifurcation is subcritical, the induction of repetitive cycling may show hysteresis, i.e. it may not be reversed by reversing the parameter change which produced it. Then measures adequate to prevent repetitive mitosis might be inadequate to arrest an established pattern of repetitive mitosis.

As an explanation for starting and stopping repetitive mitoses, this model is undoubtedly too simple. There is little or no experimental evidence for cyclin degradation until some time after the start of M phase, so it seems doubtful that subtle changes in cyclin degradation rate regulate the triggering of M phase. In living cells, the presence of checkpoints suggests that there are ways other than Hopf bifurcation to control repetitive cycling. Novak and Tyson [14] have modeled checkpoints as 'stable steady state[s] inserted into and removed from the cell cycle by saddle-node bifurcations' (Tyson, personal communication). Their bifurcations occur in a subsystem whose bifurcation parameters are really state variables in a more complete mechanism of cell cycle control. The complete system is too complicated to analyze here, but it would seem that the change between cycling and checkpoint-arrested behavior in the complete system may be due to something like a saddle-node bifurcation on a loop ([21], p. 401), i.e. on the limit cycle of the complete system. The concept of checkpoints does not replace the concept of a limit cycle, however. Repetitive cycling, with

checkpoints, would seem to require an underlying limit cycle, which might be controlled sometimes by Hopf bifurcation, and sometimes by saddle-node bifurcation on the limit cycle.

In the previous model [15] the protein Suc1, which binds M and inhibits autocatalysis, was assigned the role of B, and this accounted qualitatively for the known effects of Suc1 on M activation. The role was dynamically essential for the generation of oscillations, just as it is essential here for bistability. There was a problem in accounting for the inhibition of autocatalysis by Suc1, because Suc1 does not inhibit the histone H1 kinase activity of M [18,45,46], so there is reason to think that it may likewise fail to inhibit the hyperphosphorylation (activation) of Cdc25. Therefore the autocatalytic activation of M was attributed to a complex of M and Cdc25 which catalyzed the activation of M, and which was inactivated by binding to Suc1. There is some evidence for such a complex [19]. However, evidence is accumulating that the main route of autocatalysis is through M-catalyzed hyperphosphorylation of Cdc25 [47,48]. Accordingly, in the course of the present work, the question was considered whether the role of Suc1 could be explained by a two-stage process, with an initial 'priming' stage (formation of a complex inhibited by Suc1) triggering a second, larger stage (Suc1-independent hyperphosphorylation of Cdc25 by M). The first stage would contribute Suc1-sensitivity and the resulting dynamics, while the second stage would provide amplification. It was found, however, that a Suc1-sensitive first stage was not able to control (i.e. prevent activation of) a Suc1-insensitive autocatalytic second stage of more than about the same magnitude, so the second stage added relatively little amplification. Furthermore, because of the Suc1-insensitive second stage, the system had a rather high activation rate at low M, requiring a relatively high inactivation rate. With a linear inactivation rate, this put the upper fixed point at a very incomplete level of activation. Fuller activation could be obtained with saturable inactivation kinetics (cf. Fig. 4); but the lack of significant amplification made this model appear not attractive.

Zheng and Ruderman [20] have observed that a small region of cyclin B (the 'P box') is essential for activation of M by the low-activity interphase form of Cdc25, and they have proposed a two-stage model of M activation. The first stage, dependent on the P box, is the slow activation of M by the low activity-form of Cdc25. By providing a small priming quantity of M, this 'jump starts' the much faster second stage, which is the M-induced hyperphosphorylation of Cdc25 to the high-activity form, which activates more M regeneratively. This priming process essentially corresponds to a small constant term ('e') in the model proposed previously [15], and that is the way it has been incorporated into the present model, where this term is now dependent on D. The present model assumes that Suc1, by binding to M, prevents phosphorylation of Cdc25, up to the stoichiometric M-binding capacity of Suc1, even though Suc1 does not inhibit phosphorylation of histone H1. An explanation for such selective inhibition might be that Suc1, which forms dimers and hexamers [49], may inhibit Cdc25 activation in vivo not by inhibition of the enzymatic activity of M but rather by immobilizing M and Cdc25, perhaps as part of some fixed multimeric structure, so that M and Cdc25 cannot undergo multiple interactions with each other. In that case Suc1 might show no inhibitory effect on Cdc25 phosphorylation in vitro.

Zheng and Ruderman concede that the Galaktionov–Beach complex [19] could account for the observations, and it is not the intention here to reject either model, since both give the autocatalysis needed for bistability.

In addition to Suc1, there is a new candidate for the role of B in the present models, namely a stoichiometric inhibitor of MPF recently identified in *Xenopus* extracts by T.H. Lee and M.W. Kirschner (personal communication). This inhibitor is itself inhibited by phosphorylation, and would seem to account for the lag period in Cdc2 activation by cyclin [23], and the abolition of the cyclin threshold by the phosphatase inhibitor okadaic acid. Since this inhibitor becomes inactivated on entry into M phase it would make the model somewhat different. Evidence for still another titratable inhibitor of mitosis has recently been reported by Kumagai and Dunphy [50].

There are several events of the cell cycle that require to be switched decisively. Hints that a mechanism like the mitotic switch (Fig. 1) may control the G_1/S transition, include the fact that Cdc25A is activated by cyclinE/Cdk2 at the G_1/S transition

[51], and the fact that the homolog of Suc1 in *S. cerevisiae* (Cks1) appears to be active at the G_1/S transition as well as at G_2/M [52]. Also a number of cyclin-dependent kinase (Cdk) inhibitors (CKIs) have been described [53–56]; and Nasmyth and Hunt [53] have suggested that the Cdks 'build up like water behind a CKI dam,' which eventually bursts, releasing a flood of active Cdks which irrevocably commit the cell to the next phase of the cell cycle. The present model is essentially a mathematically explicit model of such a 'dam,' which illustrates the role that bistability and saddle-node bifurcation may play in controlling progress through the cell cycle.

The Cdk inhibitor Far1 has been suggested to act in a positive-feedback loop [57], in a role similar to that of B in the present model. Also Xiong et al. [58] found that titration of cyclin A/Cdk2 with the inhibitor $p21^{WAF1/CIP1}$ formed increasing amounts of cyclin A/Cdk2/p21 ternary complexes, but did not inhibit the kinase activity of cyclin A/Cdk2 until nearly a stoichiometric amount was added, and then gave abrupt and complete inhibition. A similar effect, due to hysteresis, occurs in the present model when the inhibitor B is added to a system initially in the high-activity stable steady state (Fig. 8): there is no inactivation of M until a critical amount of B has been added, at which point a saddle-node bifurcation occurs and there is abrupt inactivation. However it is not known whether this could be the explanation for the observations of Xiong et al. A somewhat similar hysteresis experiment with graded inhibition by partial cyclin destruction (instead of titration with an inhibitor) has been proposed by Novak and Tyson [12].

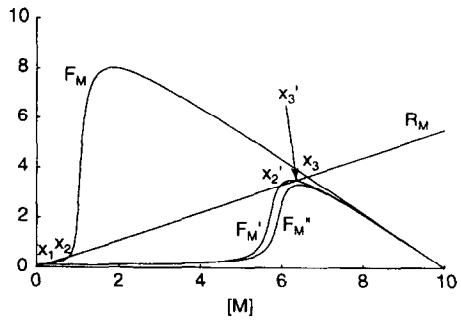

Fig. 8. Inactivation by addition of inhibitor B. $\mathbf{F}_M$ and $\mathbf{R}_M$ are the same as Fig. 2A, $B = 1$. If the system is initially at the high-activity fixed point ($\mathbf{x}_3$), increasing B to 5.7 ($\mathbf{F}'_M$) moves the unstable fixed point ($\mathbf{x}'_2$) close to the high-activity fixed point, but the system stays at the high-activity fixed point ($\mathbf{x}'_3$), which changes very little. A further increase to $B = 5.9$ ($\mathbf{F}''_M$) obliterates the high-activity fixed point by saddle-node bifurcation, and causes abrupt inactivation.

References

[1] A.W. Murray, Curr. Biol., 3 (1993) 291.
[2] M.J. Solomon, Curr. Opin. Cell Biol., 5 (1993) 180.
[3] A.W. Murray and T. Hunt, The Cell Cycle: An Introduction, W.H. Freeman, New York, 1993.
[4] W.G. Dunphy, Trends Cell Biol., 4 (1994) 202.
[5] M. Dorée and S. Galas, FASEB J., 8 (1994) 1114.
[6] M.S. Cyert and M.W. Kirschner, Cell, 53 (1988) 185.
[7] C. Hyver and H. Le Guyader, BioSystems, 24 (1990) 85.
[8] R. Norel and Z. Agur, Science, 251 (1991) 1076.
[9] C.D. Thron, Science, 254 (1991) 122.
[10] J.J. Tyson, Proc. Natl. Acad. Sci. USA, 88 (1991) 7328.
[11] M.N. Obeyesekere, S.L. Tucker and S.O. Zimmerman, Biochem. Biophys. Res. Commun., 184 (1992) 782.
[12] B. Novak and J.J. Tyson, J. Theoret. Biol., 165 (1993) 101.
[13] B. Novak and J.J. Tyson, J. Cell Sci., 106 (1993) 1153.
[14] B. Novak and J.J. Tyson, J. Theoret. Biol., 173 (1995) 283.
[15] C.D. Thron, BioSystems, 32 (1994) 97.
[16] M.N. Obeyesekere, S.L. Tucker and S.O. Zimmerman, Cell Prolif., 27 (1994) 105.
[17] W.G. Dunphy, L. Brizuela, D. Beach and J. Newport, Cell, 54 (1988) 423.
[18] W.G. Dunphy and J. Newport, Cell, 58 (1989) 181.
[19] K. Galaktionov and D. Beach, Cell, 67 (1991) 1181.
[20] X.-F. Zheng and J.V. Ruderman, Cell, 75 (1993) 155.
[21] J.K. Hale and H. Koçak, Dynamics and Bifurcations, Springer-Verlag, New York, 1991.
[22] M.J. Solomon, M. Glotzer, T.H. Lee, M. Philippe and M.W. Kirschner, Cell, 63 (1990) 1013.
[23] C. Smythe and J.W. Newport, Cell, 68 (1992) 787.
[24] Z. Tang, T.R. Coleman and W.G. Dunphy, EMBO J., 12 (1993) 3427.
[25] T. Izumi and J.L. Maller, Mol. Biol. Cell, 6 (1995) 215.
[26] B. Ducommun, G. Draetta, P. Young and D. Beach, Biochem. Biophys. Res. Commun., 167 (1990) 301.
[27] S. Moreno, P. Nurse and P. Russel, Nature, 344 (1990) 549.
[28] J. Monod and F. Jacob, Cold Spring Harbour Symp. Quant. Biol., 26 (1961) 389.
[29] J.J. Tyson, J. Chem. Phys., 62 (1975) 1010.
[30] L. Edelstein-Keshet, Mathematical Models in Biology, Random House, New York, 1988.
[31] J. Lewis, J.M.W. Slack and L. Wolpert, J. Theoret. Biol., 65 (1977) 579.
[32] W.L. Kath and J.D. Murray, SIAM J. Appl. Math., 45 (1985) 943.
[33] J.D. Murray, Mathematical Biology, Springer-Verlag, Berlin, 1989.

[34] P. Gray and S.K. Scott, Chemical Oscillations and Instabilities, Clarendon Press, Oxford, 1990.
[35] A. Goldbeter and D.E. Koshland, Jr., Proc. Natl. Acad. Sci. USA, 78 (1981) 6840.
[36] M. Okamoto and K. Hayashi, J. Theoret. Biol., 104 (1983) 591.
[37] C. Walter, R. Parker and M. Ycas, J. Theoret. Biol., 15 (1967) 208.
[38] A. Arkin and J. Ross, Biophys. J., 67 (1994) 560.
[39] J. Higgins, Ind. Eng. Chem., 59(5) (1967) 18.
[40] C.D. Thron, Bull. Math. Biol., 53 (1991) 383.
[41] C.D. Thron, Biophys. Chem., 46 (1993) 187.
[42] R. FitzHugh, Biophys. J., 1 (1961) 445.
[43] J. Rinzel and B. Ermentrout, in C. Koch and I. Segev (Editors), Methods of Neuronal Modeling, The MIT Press, Cambridge, MA, 1989, p. 135.
[44] R. FitzHugh, J. Gen. Physiol., 43 (1960) 867.
[45] L. Brizuela, G. Draetta and D. Beach, EMBO J., 5 (1987) 3507.
[46] S. Moreno, J. Hayles and P. Nurse, Cell, 58 (1989) 361.
[47] I. Hoffmann, P.R. Clarke, M.J. Marcote, E. Karsenti and G. Draetta, EMBO J., 12 (1993) 53.
[48] T. Izumi and J.L. Maller, Mol. Biol. Cell, 4 (1993) 1337.
[49] H.E. Parge, A.S. Arvai, D.J. Murtari, S.I. Reed and J.A. Tainer, Science, 262 (1993) 387.
[50] A. Kumagai and W.G. Dunphy, Mol. Biol. Cell, 6 (1995) 199.
[51] I. Hoffman, G. Draetta and E. Karsenti, EMBO J., 13 (1994) 4302.
[52] Y. Tang and S.I. Reed, Genes Dev., 7 (1993) 822.
[53] K. Nasmyth and T. Hunt, Nature, 366 (1993) 634.
[54] T. Hunter, Cell, 75 (1993) 839.
[55] J. Pines, Trends Biochem. Sci., 19 (1994) 143.
[56] M. Peter and I. Herskowitz, Cell, 79 (1994) 181.
[57] M. Peter and I. Herskowitz, Science, 265 (1994) 1228.
[58] Y. Xiong, G.J. Hannon, H. Zhang, D. Casso, R. Kobayashi and D. Beach, Nature, 366 (1993) 701.